Bioorganic & Medicinal Chemistry 26 (2018) 3429–3437

Contents lists available at ScienceDirect

Bioorganic & Medicinal Chemistry

journal homepage: www.elsevier.com/locate/bmc

# Design, synthesis and biological evaluation of phosphopeptides as Polo-like kinase 1 Polo-box domain inhibitors

Tong-yuan Lin[a,b,c], Hong-ping Min[a,b,c], Cheng Jiang[a], Miao-miao Niu[a,b,c], Fang Yan[a,b,c], Li-li Xu[a,b,c,*], Bin Di[a,b,c,*]

[a] Jiangsu Key Laboratory of Drug Design and Optimization, China Pharmaceutical University, Nanjing 210009, China
[b] Key Laboratory on Protein Chemistry and Structural Biology, China Pharmaceutical University, Nanjing 210009, China
[c] Key Laboratory of Drug Quality Control and Pharmacovigilance, China Pharmaceutical University, Nanjing 210009, China

ARTICLE INFO

*Keywords:*
Plk1 PBD inhibitors
Improved-SPPS
Phosphopeptides
Intracellular activity
Cell membranes permeability

ABSTRACT

Polo-like kinase 1 (Plk1) is an anti-cancer target due to its critical role in mitotic progression. A growing body of evidence has documented that Peptide-Plk1 inhibitors showed high Plk1 binding affinity. However, phosphopeptides-Plk1 inhibitors showed poor cell membranes permeability, which limits their clinical applications. In current study, nine candidate phosphopeptides consisting of non-natural amino acids were rationally designed and then successfully synthesized using an Fmoc-solid phase peptide synthesis (SPPS) strategy. Moreover, the binding affinities and selectivity were evaluated via fluorescence polarization (FP) assay. The results confirmed that the most promising phosphopeptide **6** bound to Plk1 PBD with the $IC_{50}$ of 38.99 nM, which was approximately 600-fold selectivity over Plk3 PBD ($IC_{50}$ = 25.44 μM) and nearly no binding to Plk2 PBD. Furthermore the intracellular activities and the cell membrane permeability of phosphopeptide **6** were evalutated. Phosphopeptide **6** demonstrated appropriate cell membrane permeability and arrested HeLa cells cycle in G2/M phase by regulating CyclinB1-CDK1. Further, phosphopeptide **6** showed typical apoptotic morphology and induced caspase-dependent apoptosis. In conclusion, we expect our discovery can provide new insights into the further optimization of Plk1 PBD inhibitors.

## 1. Introduction

Members of the Polo subfamily of protein kinases (collectively, Plks), a conserved member of serine/threonine protein kinases family, were identified in *Drosophila* and regarded as a primary regulator in multiple stages of mitosis.[1] Till date, five Plks (Plk1, Plk2/Snk, Plk3/Fnk, Plk4/Sak,Plk5) in mammalian cells have been reported.[2] Plk1 has been well-studied in the Polo-like kinase family. The overexpression of Plk1 has been observed in a broad spectrum of tumor cells, but not in normal cells, and is also associated with adverse prognosis, metastatic potential and cancer progression. Furthermore, much evidence has also documented that the overexpression of Plk1 inactivates Cyclin-Dependent Kinases (CDK-1) in a Cell division Cyclin 25 homolog C (CdC25C)-dependent manner.[3] However, Plk3 is other one closely related kinases with Plk1 which regards as negative regulators responsible for the inhibition of cell cycle progression and tumor cell development at multiple stages of mitosis.[4] Hence, the development of Plk1-specific inhibitors is critically necessary for the treatment of Plk1-related cancer to avoid the potential side effects caused by poor selectivity.

Structurally, Plk1 is characterized by the presence of conserved N-terminal kinase domain (KD), C-terminal domain consisting of two "polo boxes domain" (PBD) and the connecting region in the middle (interdomain linker, IDL) (Fig. 1).[5] The PBD contains two structurally-related PB1 and PB2 motifs, and the groove between PB1 and PB2 mediates protein-protein interactions (PPI) by binding to the phosphoserine (pSer)/phosphothreonine (pThr).[6–9]

Over the past few decades, much attention was devoted to produce several Plk1 PBD inhibitors (poloxin, poloxipan, purpurogallin, rigosertib phosphopeptides and so on), which exhibits a high specificity to the PBD of Plk1. Furthermore, many of these small molecule Plk1 PBD inhibitors have ongoing in different phase of clinical trials.[10–14] However, phosphopeptides-Plk1 inhibitors showed poor cell membranes permeability, which hampered its successful application in clinic.

Therefore, based on the 10 mer-peptide 1 (PLHSpTAIYAD), 9-mer peptide 2 (Ac-FDPPLHSpTA) and the crystal structure of Plk1 PBD,[15–20] efforts were made to design a series of potential non-ATP-competitive phosphopeptides targeting the Plk1 PBD. Then nine candidate phosphopeptides were successfully synthesized through Fmoc-solid phase

* Corresponding authors at: Jiangsu Key Laboratory of Drug Design and Optimization, China Pharmaceutical University, Nanjing 210009, China.
*E-mail addresses:* 1620174420@cpu.edu.cn (L.-l. Xu), dibin@cpu.edu.cn (B. Di).

https://doi.org/10.1016/j.bmc.2018.05.014
Received 5 April 2018; Received in revised form 7 May 2018; Accepted 10 May 2018
Available online 14 May 2018

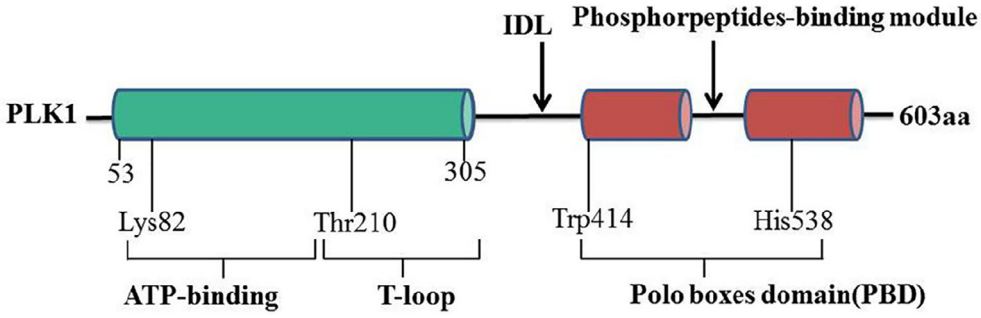


**Fig. 1.** Structural domains of human Plk1.

peptide synthesis method.

Notably, the competitive binding assay based on fluorescence polarization techniques (FP) was used to measure the abilities of the phosphopeptides to compete with fluorescently labeled probes of pThr-containing peptides for binding to Plk1 PBD. Next, we systematically evaluated the binding selectivity of phosphopeptides to the PBD of Plk1 relative to the PBD of Plk2 and Plk3. The results suggested that these phosphopeptides not only exhibited considerably high binding affinities to Plk1 PBD at low nanomolar concentrations, but also had specific selectivity for Plk1 PBD. It is worth noting that the most potential phosphopeptide **6** showed strong binding-affinity with the $IC_{50}$ of 38.99 nM, yet retained good selectivity for Plk1 PBD relative to the PBD of Plk2 and Plk3. In addition, *in vitro* biological assays revealed that phosphopeptide **6** blocked cell cycle progression of G2/M phase in a time and concentration-dependent manner and induced apoptosis in a concentration-dependent manner. Moreover, western blot analysis showed that treatment of HeLa cells with phosphopeptide **6** significantly increased the protein cleavage of caspase-3 and PARP and concentration dependently decreased the expression of cyclin B1 and CDK1. Laser scanning confocal microscopy (LSCM) verified the fact that the phophorpeptide **6** could penetrate cell membranes into the cytoplasm.

## 2. Results and discussion

### 2.1. Chemicals

In our current study, we developed a more efficient peptide solid-phase synthesis route to produce phosphopeptides comprising of non-natural amino acids. These candidate phosphopeptides were successfully synthesized using different coupling reagents with double or triple coupling reactions for non-natural amino acids and novel deprotection solutions for the Fmoc protecting groups.

One possible explanation could be that the use of different coupling reagents in secondary coupling reactions may affect the solvation state of Rink amide resin and phosphopeptide, which makes the Rink amide resin and phosphopeptide tend to extend as well as be exposed to more binding sites. It is known that the 25% piperidine-DMF has been chosen as deprotection solution in the conventional Fmoc-solid phase peptide synthesis. Specially, in our current study, 25% piperidine-DMF-0.1 M Hydroxybenzotriazole (HOBT) solution was adopted as a novel deprotection solution. In particular, Asp was followed by Pro in phosphopeptide sequence. The major advantage of 25% piperidine-DMF-0.1 M HOBT solution is to avoid the aspartimide formation during the deprotection of Fmoc protection group. These crude phosphopeptide were then purified via preparative Reverse Phase High-Performance Liquid Chromatography (RP-HPLC) C18 columns. As can be seen from Table 1, the relative molecular weights of these phosphopeptide were comparable to the theoretical values, with a purity greater than 95% (support information Fig. S1 and Fig. S2). In sum, these results provide important insights on the preparation of phosphopeptides containing non-natural amino acids with spatial steric hindrance.

**Table 1**
The ESI-Mass Spectral Data and HPLC Purity of Synthetic phosphopeptides.

| No | Sequence | Theoretical $[M+H]^+$ | Observed $[M+2H]^{2+}$ | HPLC Purity (%) |
|---|---|---|---|---|
| **1** | Ac-FDPPLHSpTAIYAN-$NH_2$ | 1581.71 | 790.86 | 95.03 |
| **2** | Ac-QTF(4-Cl)DPPLHSpTAIYAN-$NH_2$ | | 915.39 | 95.10 |
| **3** | Ac-QTF(4-F)DPPLHSpTAIYAN-$NH_2$ | 1814.79 | 907.40 | 95.07 |
| **4** | Ac-QTF(4-$NO_2$)DPPLHSpTAIYAN-$NH_2$ | 1841.78 | 920.90 | 96.11 |
| **5** | Ac-QTF(4-$OCH_3$)DPPLHSpTAIYAN-$NH_2$ | 1826.98 | 913.49 | 95.78 |
| **6** | Ac-QTF(3,4-Cl)DPPLHSpTAIYAN-$NH_2$ | 1865.72 | 933.36 | 95.04 |
| **7** | Ac-TF(3,4-Cl)DPPLHSpTAIYAN-$NH_2$ | 1737.00 | 869.32 | 96.31 |
| **8** | Ac-QF(3,4-Cl)DPPLHSpTAIYAN-$NH_2$ | 1765.06 | 883.52 | 95.54 |
| **9** | Ac-F(3,4-Cl)DPPLHSpTAIYAN-$NH_2$ | 1636.61 | 818.81 | 95.26 |

### 2.2. Binding affinity and selectivity of phosphopeptides with Plk1 PBD, Plk2 PBD and Plk3 PBD

On the basis of the 10 mer-peptide 1 (PLHSpTAIYAD) and 9-mer peptide 2 (Ac-FDPPLHSpTA), the phosphopeptide **1** (Ac-FDPPLHASpTAIYAN-$NH_2$) was used as the template in the current study. We systematically evaluated the binding affinity of these phosphopeptides to Plk1 PBD using our optimized FP binding assay. Significantly, the binding-affinity data in Table 2 illustrated that there were obvious differences in the binding of these phosphopeptides to Plk1 PBD, Plk2 PBD and Plk3 PBD. The FP findings showed that the

**Table 2**
Binding affinity and selectivity of phosphopeptides for Plk1 PBD, Plk2 PBD and Plk3 PBD ("–" represent to the no binding-affinities).

| No. | Sequence | Plk1 PBD ($IC_{50}$) | Plk2 PBD ($IC_{50}$) | Plk3 PBD ($IC_{50}$) |
|---|---|---|---|---|
| **1** | Ac-FDPPLHSpTAIYAN-$NH_2$ | 283.3 nM | 13.37 μM | – |
| **2** | Ac-QTF(4-Cl)DPPLHSpTAIYAN-$NH_2$ | 90.12 nM | – | – |
| **3** | Ac-QTF(4-F)DPPLHSpTAIYAN-$NH_2$ | 74.14 nM | – | – |
| **4** | Ac-QTF(4-$NO_2$)DPPLHSpTAIYAN-$NH_2$ | 70.24 nM | – | – |
| **5** | Ac-QTF(4-$OCH_3$)DPPLHSpTAIYAN-$NH_2$ | 2.109 μM | – | – |
| **6** | Ac-QTF(3,4-Cl)DPPLHSpTAIYAN-$NH_2$ | 38.99 nM | – | 25.44 μM |
| **7** | Ac-TF(3,4-Cl)DPPLHSpTAIYAN-$NH_2$ | 75.27 nM | – | – |
| **8** | Ac-QF(3,4-Cl)DPPLHSpTAIYAN-$NH_2$ | 65.59 nM | – | – |
| **9** | Ac-F(3,4-Cl)DPPLHSpTAIYAN-$NH_2$ | 78.42 nM | 0.7157 μM | – |